

Stepwise Functionalization of ZnO Nanotips with DNA

Olena Taratula, Elena Galoppini,* and Richard Mendelsohn

Department of Chemistry, Rutgers, The State University of New Jersey, 73 Warren Street,
Newark, New Jersey 07102

Pavel Ivanoff Reyes, Zheng Zhang, Ziqing Duan, Jian Zhong, and Yicheng Lu

Department of Electrical and Computer Engineering, Rutgers, The State University of New Jersey,
Piscataway, New Jersey 08854

Received August 18, 2008. Revised Manuscript Received November 27, 2008

A surface functionalization methodology for the development of ZnO nanotips biosensors that can be integrated with microelectronics was developed. Two types of long chain carboxylic acids linkers were employed for the functionalization of 0.5 μm thick MOCVD-grown ZnO nanotip films with single-stranded DNA (ssDNA), followed by hybridization with complementary ssDNA tagged with fluorescein. The ZnO functionalization strategy was developed for the fabrication of ZnO nanotips-linker-biomolecule films integrated with bulk acoustic wave (BAW) biosensors, and it involved three main steps. First, 16-(2-pyridyldithiol)hexadecanoic acid or *N*-(15-carboxypentadecanoyloxy)succinimide, both bifunctional C16 carboxylic acids, were bound to ZnO nanotip films through the COOH group, leaving at the opposite end of the alkyl chain a thiol group protected as a 2-pyridyl disulfide, or a carboxylic group protected as a *N*-succinimide, respectively. In the second step, ssDNA was covalently linked to each type of ZnO-linker film: the 2-pyridyl disulfide end group was substituted with 16 bases 5'-thiol-modified DNA (SH-ssDNA), and the *N*-succinimide ester end group was substituted with 16 bases 5'-amino-modified DNA (NH₂-ssDNA). In the third step, the DNA-functionalized ZnO nanotip films were hybridized with complementary 5'-fluorescein ssDNA. The surface-modified ZnO nanotip films were characterized after each step by FT-IR-ATR, fluorescence emission spectroscopy, and fluorescence microscopy. This functionalization approach allows sequential reactions on the surface and, in principle, can be extended to numerous other molecules and biomolecules.

Introduction

Zinc Oxide (ZnO) is an n-type, wide band gap ($E_g = 3.35$ eV) semiconductor that can be grown to form highly anisotropic nanostructures on numerous substrates including sapphire, glass, silicon, and conductive surfaces (ITO, gold).¹ In recent years, highly ordered, “nail-bed” ZnO nanocrystal layers called “nanotips” films, also called nanorods or nanowires depending on their shape,^{2,3} have found applications in a variety of devices including sensors.^{1,4} ZnO exhibits a variety of properties, including piezoelectricity, that make it well suited for chemical and biochemical sensing. For instance, ZnO can be integrated with bulk acoustic microwave (BAW)⁵ and quartz crystal microbalance (QCM)⁶ sensors to detect gases and liquids, such as CH₄, CO, H₂, amines, ethanol, and NO₂.^{7–10} In addition, ZnO

is a biocompatible oxide,¹¹ and it has been shown that ZnO nanotips are compatible with intracellular material.¹² There are considerable advantages in developing sensors from ZnO nanotip films. As compared to planar configurations (epitaxial films), ZnO nanotips have a huge surface area available to bind the analyte. Indeed, sensors prepared from ZnO nanotips exhibited faster response and higher sensitivity than did those with the epitaxial ZnO.¹³ More recently, it has been demonstrated that ZnO nanotip films can be made reversibly hydrophilic or hydrophobic by UV treatment or oxygen annealing, respectively,¹⁴ and that the minimum volume of aqueous samples required for BAW sensors prepared from hydrophilic ZnO nanotips was dramatically decreased after the UV treatment.¹² In summary, the photophysical properties of ZnO combined with the nail-bed morphology lead to novel and versatile materials for sensing applications.

A major limitation to developing new applications for ZnO nanotips, not only for sensors but for any kind of device, is that there are only a few methods available to functionalize the surface of ZnO nanotips. The functionalization step is critically important

* Corresponding author. E-mail: galoppin@rutgers.edu.

(1) Özgür, Ü.; Alivov, Ya. I.; Liu, C.; Teke, A.; Reshchikov, M. A.; Doğan, S.; Avrutin, V.; Cho, S.-J.; Morkoç, H. *J. Appl. Phys.* **2005**, *98*, 041301.

(2) Heo, Y. W.; Norton, D. P.; Tien, L. C.; Kwon, Y.; Kang, B. S.; Ren, F.; Pearton, S. J. *Mater. Sci. Eng.* **2004**, *47*, 1.

(3) (a) Greene, L. E.; Yuhas, B. D.; Law, M.; Zitoun, D.; Yang, P. *Inorg. Chem.* **2006**, *45*, 7535. (b) Cui, J.; Gibson, U. J. *J. Phys. Chem. B* **2005**, *109*, 22074.

(4) Ellmer, K.; Klein, A.; Rech, B., Eds. *Transparent Conductive Zinc Oxide: Basics and Applications in Thin Film Solar Cells*; Springer Series in Materials Science; Springer: New York, 2008; Vol. 104.

(5) (a) Gabl, R.; Green, E.; Schreiter, M.; Feucht, H. D.; Zeininger, H.; Primig, R.; Pitzer, D.; Eckstein, G.; Wersing, W.; Reichl, W.; Runck, J. *Proc. IEEE Sens. Technol. Lett.* **2004**, *42*, 505.

(6) Zhang, Z.; Chen, H.; Zhong, J.; Chen, Y.; Lu, Y. *Proc. IEEE Int. Freq. Control Symp.* **2006**, 545.

(7) Anisimkin, V. I.; Penza, M.; Valentini, A.; Quaranta, F.; Vasanelli, L. *Sens. Actuators, B* **1995**, *23*, 197.

(8) Liao, L.; Lu, H. B.; Liu, C.; Fu, D. J.; Liu, Y. L. *Appl. Phys. Lett.* **2007**, *91*, 173110.

(9) Weissenrieder, K.; Mueller, S. J. *Thin Solid Films* **1997**, *300*, 30.

(10) Koch, M. H.; Timbrell, P. Y.; Lamb, R. N. *Semicond. Sci. Technol.* **1995**, *10*, 1523.

(11) (a) Miller, B. G.; Traut, T. W.; Wolfenden, R. V. *J. Am. Chem. Soc.* **1998**, *120*, 2666. (b) Look, D. C.; Hemsley, J. W.; Sizelove, J. R. *Phys. Rev. Lett.* **1999**, *82*, 2552. (c) Muthukumar, S.; Chen, Y.; Zhong, J.; Cosandey, F.; Lu, Y.; Siegrist, T. *J. Cryst. Growth* **2004**, *261*, 316. (d) Muthukumar, S.; Zhong, J.; Chen, Y.; Lu, Y.; Siegrist, T. *Appl. Phys. Lett.* **2003**, *82*, 742. (e) Zhang, J.; Zhang, Z.; Wang, T. *Chem. Mater.* **2004**, *16*, 768.

(12) Hilli, S. M.; Al-Mofarji, R. T.; Willander, M. *Appl. Phys. Lett.* **2006**, *89*, 173119.

(13) (a) Tian, Z. R.; Voigt, J. A.; Liu, J.; McKenzie, B.; McDermott, M. J.; Rodriguez, M. A.; Konishi, H.; Xu, H. *Nat. Mater.* **2003**, *2*, 821. (b) Yi, G.-C.; Wang, C.; Park, W. I. *Semicond. Sci. Technol.* **2005**, *20*, S22.

(14) Zhang, Z.; Chen, H.; Zhong, J.; Saraf, G.; Lu, Y. *TMS IEEE J. Electron. Mater.* **2007**, *36*, 895.

for the realization of ZnO-based sensor technology with high sensitivity and selectivity. In fact, there have been only a few reports on the direct functionalization of nanostructured ZnO surfaces with biomolecules.¹⁵ The covalent binding, in a controlled and well-defined manner, of large biomolecules that carry numerous polar groups, such as proteins, DNA, or enzymes, to ZnO nanostructured films is a challenge. Physisorption, aggregation, and formation of a disordered layer are likely to occur.¹⁶

This Article describes a stepwise ZnO functionalization methodology that allows sequential reactions on the surface of ZnO nanotips. While the functionalization sequence described in this Article was designed for the development of biosensors that can be integrated with microelectronics, the methodology can be useful for numerous other applications that require the binding of molecules to ZnO. In previous work with ZnO nanotip films, we investigated methods of functionalization of ZnO surfaces with a variety of small molecules and sensitizing dyes.^{17,18} This work indicated that the COOH and Si(OMe)₃ groups binds covalently to the surface, while others (thiols) do not.¹⁷ Second, it was observed that with ZnO nanocrystalline materials, nanoparticles as well as nanotips, it is important to control the binding experimental conditions, because ZnO is easily dissolved by strong acids. For instance, pH conditions must be controlled ($4 < \text{pH} < 9$) to avoid etching of the ZnO nanotips layers.¹⁵ MgZnO nanotip films showed instead an improved resistance to acids.¹⁵

On the basis of these results, we have now used long chain bifunctional linkers that bind to ZnO with a carboxylic group leaving a surface “reactive layer” capped with an end group that can form a covalent bond with the biomolecule. The approach is similar to that used for the self-assembling of monolayers (SAMs) on gold,¹⁹ although we do not anticipate that on ZnO nanotips the chains would be as ordered or as closely packed. The function of the “reactive layer” is to ensure the controlled immobilization of biomolecules to the layer through a covalent bond, to avoid crowding, and to provide a more stable and uniform interface that is less prone to etching and that can undergo further reactions. For the purpose of sensing, a direct contact of the biomolecule with the ZnO surface is not necessary, as detection of a remotely attached biomolecule can be performed through a variety of methods using sensors such as a QCM or optical methods, that is, fluorescence emission, for instance. The binding and hybridization of DNA here described was selected as a proof-of-concept experiment to test the formation of a ZnO-layer-biomolecule surface and to determine whether sequential reactions and hybridization procedures were possible on such layer. This method was recently repeated to prepare two functioning biosensing devices: a ZnO nanotips-based quartz crystal microbalance²⁰ and a multifunctional ZnO-based thin film bulk

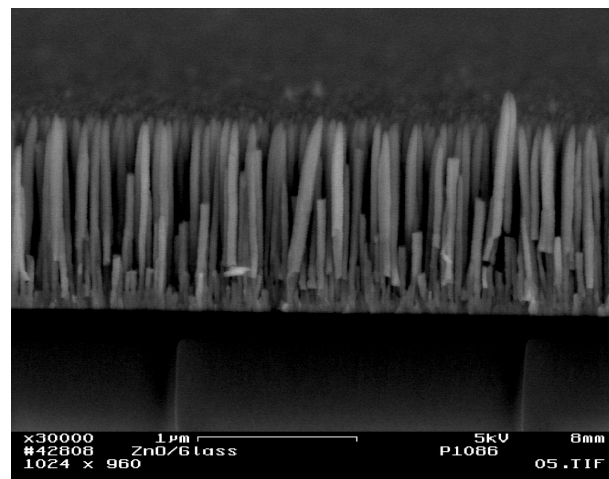


Figure 1. FESEM image of ZnO nanotips grown on glass substrate by MOCVD method.

acoustic resonator,²¹ and the details for these devices' preparation and testing will be published elsewhere.

Results and Discussion

The ZnO nanotips used for the functionalization experiments were grown on glass or c-sapphire substrates using the metalorganic chemical vapor deposition (MOCVD) method already described.^{16,22} Briefly, diethylzinc and oxygen were used as the metalorganic Zn source and oxidizer, respectively. The substrate temperature was kept at $\sim 475^\circ\text{C}$, and the chamber pressure was maintained at around 50 Torr during the growth. The ZnO nanotips are *c*-axis oriented single crystals that are aligned along the direction perpendicular to the substrate. The nanotips are approximately $0.7\ \mu\text{m}$ in height, 60–80 nm in diameter, and 5–10 nm in diameter at the top. The average space between adjacent tips is more than 10 nm. A field emission scanning microscope (FESEM) image of a ZnO nanotips film used in this study is shown in Figure 1.

Two DNA immobilization methods were employed, as illustrated in Scheme 1. In both cases, a bifunctional carboxylic acid was first anchored to the MOCVD-grown ZnO nanotip films surface by the COOH group, leaving a second reactive functional group, temporarily protected to avoid unwanted reactions, available for reaction with DNA. In route A, the surface functionalized with pyridyl disulfide was reacted with thiol-modified 16 base ssDNA, and in route B, the *N*-hydroxysuccinimide-ester end group was reacted with amino-modified 16 base ssDNA. The DNA-functionalized ZnO nanotip films were hybridized with complementary 5'-fluorescein-modified ssDNA. The fluorescent tag (fluorescein) was used here only for characterization purposes, but for future biosensor applications tag-free biomolecules can be used.

DNA Immobilization via PDHA Layer (Route A). Bifunctional carboxylic acid 16-(2-pyridylthiol)hexadecanoic acid (PDHA) was bound to ZnO nanotip films by immersing the films in 2 mM solutions of the acid in 1-butanol/ethanol, as described in the Experimental Section. The binding was monitored by FTIR-ATR of the films, Figure 2a, although the intensity of spectra obtained from ZnO nanotip layers that are only $\sim 0.7\ \mu\text{m}$ thick

(15) (a) Dorfman, A.; Kumar, N.; Hahn, J.-I. *Langmuir* **2006**, *22*, 4890. (b) Kumar, N.; Dorfman, A.; Hahn, J.-I. *Nanotechnology* **2006**, *17*, 2875. (c) Zhang, Z.; Chen, H.; Zhong, J.; Chen, Y.; Lu, Y. *Proc. IEEE Int. Freq. Control Symp.* **2006**, 545. (d) Zhao, J.; Wu, L.; Zhi, J. *J. Mater. Chem.* **2008**, *18*, 2459.

(16) Chen, H.; Zhong, J.; Saraf, G.; Zhang, Z.; Lu, Y.; Fetter, L. A.; Pai, C. S. *Proc. SPIE* **2004**, 5592–31, 164.

(17) Taratula, O.; Galoppini, E.; Wang, D.; Chu, D.; Zhang, Z.; Chen, H.; Saraf, G.; Lu, Y. *J. Phys. Chem. B* **2006**, *110*, 6506.

(18) Galoppini, E.; Rochford, J.; Chen, H.; Saraf, G.; Lu, Y.; Hagfeldt, A.; Boschloo, G. *J. Phys. Chem. B* **2006**, *110*, 16159.

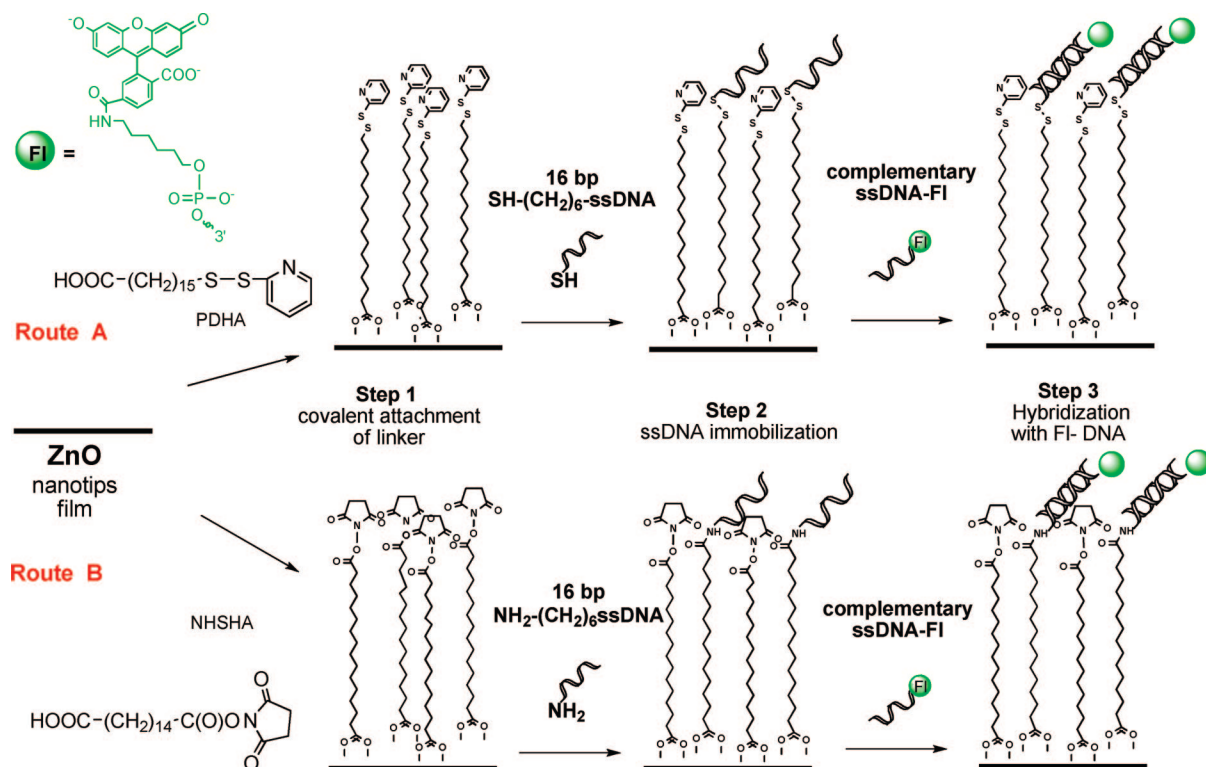
(19) Love, J. C.; Estroff, L. A.; Kriebel, J. K.; Nuzzo, R. G.; Whitesides, G. M. *Chem. Rev.* **2005**, *105*, 1103.

(20) (a) Zhang, Z.; Chen, H.; Zhong, J.; Chen, Y.; Lu, Y. *Proc. IEEE Int. Freq. Control Symp.* **2006**, 545. (b) Reyes, P. I.; Zhang, Z.; Duan, Z.; Zhong, J.; Saraf, G.; Lu, Y.; Taratula, O.; Galoppini, E.; Boustany, N. N. *IEEE Sensors* **2009**, submitted for publication.

(21) (a) Lu, Y.; Chen, Y.; Zhang, Z. Multifunctional biosensor based on ZnO nanostructures. U.S. Patent 20070210349, 2007. (b) Chen, Y.; Reyes, P. I.; Duan, Z.; Saraf, G.; Lu, Y.; Taratula, O.; Galoppini, E. *J. Vacuum Sci. Technol.* **2009**, submitted for publication.

(22) Zhong, J.; Saraf, G.; Muthukumar, S.; Chen, H.; Chen, Y.; Lu, Y. *TMS IEEE J. Electron. Mater.* **2004**, *33*, 654.

Scheme 1. ZnO Nanotips Surface Modification via Route A (Thiol–Disulfide Exchange Reaction) and Route B (NHS-Ester Hydrolysis)



is typically low. After the linker binding step (step 1 in Scheme 1), the FTIR-ATR spectrum showed the characteristic $\nu(\text{C}-\text{H})$ bands of the long saturated alkyl chain in the 3000 cm^{-1} region. The disappearance of the $\nu_{\text{as}}(\text{C}=\text{O})$ band at 1707 cm^{-1} , which is present in the spectrum of neat PDHA, and the appearance of broad bands in the $\sim 1600\text{--}1400\text{ cm}^{-1}$ region upon binding to ZnO nanotips were indicative of binding through carboxylate bonds. Such spectral changes are consistent with those observed when COOH groups bind to ZnO nanotips or ZnO nanoparticles.¹⁵

Reaction of the pyridyl disulfide with an aqueous solution of 16 bases 5'-thiol-modified ssDNA (GTGTTAGCCTCAAGTG), deprotected prior to use by reaction with a DTT-resin, in PBS buffer (phosphate buffer saline, pH 7.4) (step 2, Scheme 1) resulted in a thiol–disulfide exchange reaction. The covalent attachment of ssDNA to the alkyl chain was monitored by FTIR-ATR (Figure 2b, green line). The spectrum showed the presence of the alkyl layer together with changes in the $\sim 1200\text{ cm}^{-1}$ region assigned to the phosphate groups, and new broad bands overlapping in the $1600\text{--}1700\text{ cm}^{-1}$ region. These new bands intensified after the hybridization step.

The hybridization step to form dsDNA-functionalized ZnO nanotip films (step 3, Scheme 1) was performed by immersing the DNA-substituted ZnO films in an aqueous solution of complementary FI-ssDNA in a pH 7.4 buffer (PBS). Buffers with binding groups that could displace the layer anchored to ZnO were avoided.²³ The hybridization step was monitored by

fluorescence emission spectra ($\lambda_{\text{ex}} = 490\text{ nm}$), by detecting the presence of the fluorescent label (fluorescein), which was attached to the complementary DNA (cDNA) strand (Figure 3). The ZnO nanotips modified with ssDNA after step 2 did not fluoresce (Figure 3, black line). The fluorescence spectrum of the ZnO-N film after hybridization with FI-ssDNA (step 3, Scheme 1) shown in Figure 3 as a red dotted line indicated the presence of the FI-labeled DNA, and the fluorescence λ_{max} (520 nm) was identical to that of the free FI-ssDNA. The fluorescence emission spectrum of a ssDNA-FI solution in PBS buffer is shown as the reference in Figure 3.²⁴ It should be noted that a quantitative (concentration) comparison of absorption or emission between solution data and the data obtained from the dyes on the films is not possible. The emission λ_{max} did not shift upon binding.

To determine whether the use of the bifunctional linker is essential for DNA immobilization on the ZnO nanotip films surface and for selective hybridization, fluorescence was measured after different combinations of steps 1–3. Specifically, we prepared and measured the fluorescence of ZnO nanotip films with (a) the linker layer only (after step 1, route A), (b) linker + ss-DNA (after step 2), (c) linker + ss-DNA-FI without the ssDNA step, and (d) ZnO + ss-DNA-FI, in each case using the same binding conditions and concentrations as indicated in the Experimental Section. The control experiment was done on two types of substrates: c-sapphire (Figure 4a–d) and glass (Figure 5a–d). Only the films with properly immobilized and hybridized

(23) Phosphate buffer saline (PBS) was selected over other buffers commonly used in this kind of step that contain COOH or other functional groups, which can displace the linker layer by binding to the ZnO nanotip films surface. Indeed, we observed competitive displacement of the linker layers in the presence of EDTA (ethylene diamine tetraacetic acid) and HEPES (4-(2-hydroxyethyl)-1-piperazineethanesulfonic acid), which are buffers commonly used in these reactions. An additional advantage of PBS is that it is isotonic and non-toxic to cells, properties that could be useful for future biosensing applications. In route B, buffers containing primary amines, such as TRIS (tris(hydroxymethyl)aminomethane hydrochloride), or glycine buffers were avoided, because they contain amino groups that could compete with the amino group present on the ssDNA.

(24) The observation of fluorescence emission may suggest that the fluorophore (or a part of the fluorophore) is not in direct contact with the ZnO surface. The bandgap of ZnO is similar to that of TiO_2 , and fluorescein acts as a sensitizer of TiO_2 nanoparticles, with ultrafast injection dynamics; see, for instance: Ramakrishna, G.; Das, A.; Gosh, H. N. *Langmuir* **2004**, *20*, 1430. Hingendorff, M.; Sundström, V. *J. Phys. Chem. B* **1998**, *102*, 10. It has also been reported that fluorescein-based model compounds sensitize ZnO/SnO cells effectively: Hattori, S.; Hasobe, T.; Ohkubo, K.; Urano, Y.; Umezawa, N.; Nagano, T.; Wada, Y.; Yanagida, S.; Fukuzumi, S. *J. Phys. Chem. B* **2004**, *108*, 15200. Our attempt to bind fluorescein to the ZnO nanotip films directly resulted in some etching of the materials and uncertainty about the binding, and for this reason we were not able to verify this observation in a quantitative manner.

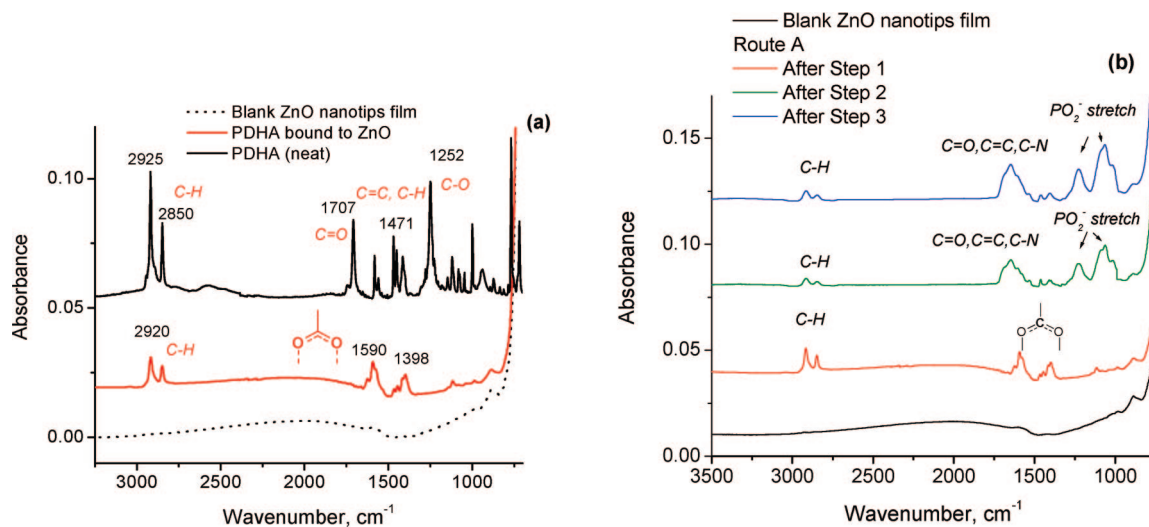


Figure 2. FTIR-ATR spectra of ZnO nanotips modification process, route A: (a) blank ZnO (bottom, dotted line), PDHA bound to ZnO nanotips (middle, red solid line), and PDHA free (top, black solid line), and (b) blank ZnO (black line), PDHA bound to ZnO (red line), immobilization of SH-ssDNA (green line), and hybridization with FI-ssDNA (blue line).

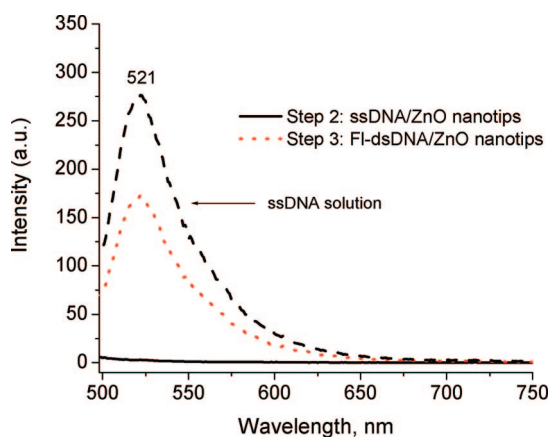


Figure 3. Route A: Fluorescence emission spectra of 25 μ M ssDNA-FI in 10 mM aqueous PBS buffer (dashed) and ZnO-N modified with SH-(CH₂)₆-ssDNA (black solid line) and ZnO-N after hybridization step with 25 μ M ssDNA-FI in 10 mM aqueous PBS buffer (red dotted line). $\lambda_{\text{ex}} = 490$ nm.

DNA that were prepared following the entire sequence indicated in Scheme 1 (steps 1, 2, and 3) were fluorescent as shown in Figures 4 and 5. This behavior was observed for both functionalization routes, A and B.

The quality of the films depended markedly on the substrate on which the ZnO nanotip films were grown, as shown by a comparison between films shown on c-sapphire and glass (Figures 4 and 5). The FESEM image of the fully functionalized nanotips grown on c-sapphire, Figure 4e, shows that the surface morphology is rough, and the nanotips are not uniformly shaped, nor perfectly aligned. This causes the binding of the DNA to be nonuniform on the corners of the rougher nanotips.

In contrast, the nanotips grown on glass are perpendicularly aligned to the normal of the surface of the glass substrate, Figure 5e. This enables the functional linkers and the immobilized and hybridized DNA to be uniformly distributed on the surface of the nanotips layer as seen from Figure 5d. This figure shows the fluorescence image of the immobilized DNA uniformly distributed all over the nanotip layers, and no aggregation or clumping has occurred.

DNA Immobilization via NHS-ssDNA Layer (Route B). In route B, a different end group was used for the fatty acid bound to ZnO

nanotips surface to react with an amino-substituted ssDNA, to demonstrate that the strategy of forming a “reactive layer” on ZnO nanotips surfaces can be extended to other functional groups and reactions. Bifunctional hexadecanoic carboxylic acid *N*-(15-carboxypentadecanoyloxy)succinimide (NHS-ssDNA) was bound by the COOH group to form a *N*-hydroxysuccinimide-ester-functionalized surface that was reacted in a substitution reaction with 16 bases 5'-amino-modified ssDNA (GTGTTAGCCT-CAAGTG) in experimental conditions similar to those reported for strategy A (Scheme 1, step 2). Finally, hybridization of the DNA-modified surface was performed with the same complementary FI-ssDNA used in strategy A (Scheme 1, step 3).

The FT-IR-ATR spectra (Figure 6a) before and after binding of NHS-ssDNA to ZnO nanotip films showed spectral changes that are consistent with the disappearance of the free COOH (C=O at 1707 cm⁻¹), the formation of carboxylate bonds, and the presence of a long alkyl chain on the metal oxide film. The $\nu_{\text{as}}(\text{C=O})$ bands assigned to the succinimide group (above 1724 cm⁻¹) remained unchanged. The spectra in Figure 6b show the changes of the ZnO layer after each step. After step 2, the spectra show bands assigned to the DNA phosphate units, and the C=O of the succinimide ester end group have been substantially diminished in intensity, suggesting that most of the end groups react, although traces of this group can be still detected. The spectra of the functionalized ZnO layers are too weak for an accurate or quantitative interpretation of the presence of unreacted end groups. Similarly, the absorption intensity of UV-vis spectra of such thin (700 nm thick) ZnO films was very weak.

Fluorescence emission spectra of the dsDNA-functionalized ZnO nanotip films indicate the presence of the fluorophore (emission $\lambda_{\text{max}} = 524$ nm) only after the hybridization step with FI-ssDNA (Figure 7). The emission intensity was lower than that observed with the films functionalized by method A, and the emission is slightly λ_{max} red-shifted as compared to the sample prepared after route A and the reference (see Figure 3), and such discrepancy may be indicative of differences in surface distribution between the two methods and possibly different interactions between chains.

(25) The small peak in the ZnO background spectrum in Figure 7 is most probably due to light scattering and is occasionally observed in clean films depending on how the data are collected.

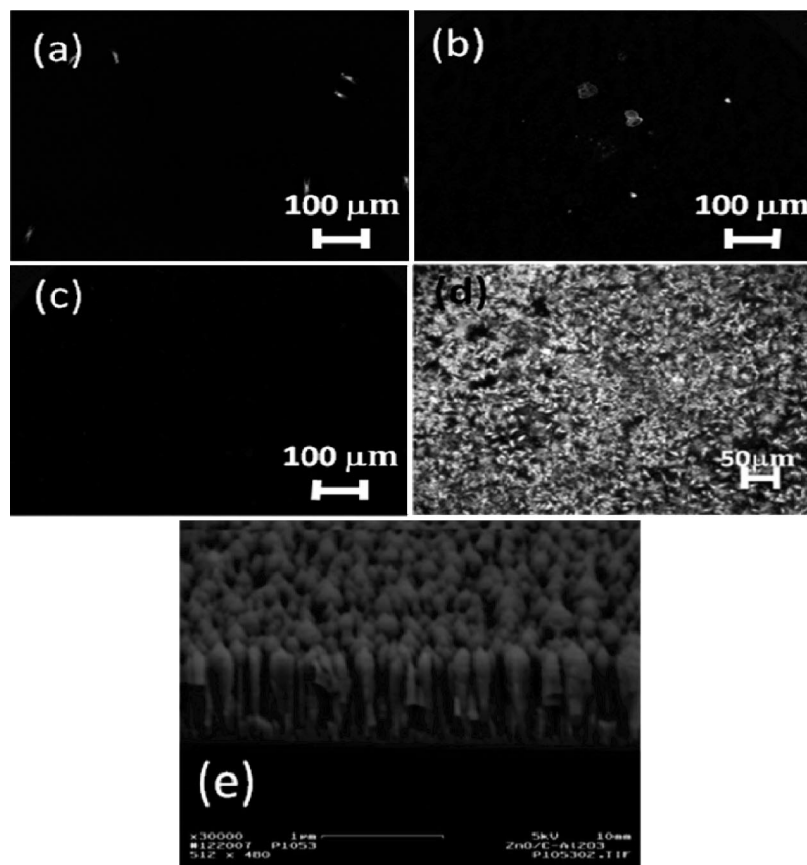


Figure 4. Fluorescence microscopy image of a ZnO nanotips film grown on c-sapphire after step 3, sequence A (image d). Only the nanotip films with properly immobilized and hybridized FI-DNA were fluorescing. No fluorescence emission was observed on films after the intermediate steps 1 (image a) and 2 (image b) and in a control experiment where a film after step 1 was treated directly with FI-ssDNA (image c). FESEM image (e) shows the surface morphology of the ZnO nanotips on c-sapphire after the entire functionalization procedure (route A).

One interesting question is where functionalization occurs, that is, whether the binding occurs primarily on the end or the sides of the ZnO nanotips. MOCVD growth methods and the proper selection of the substrate (see Figures 4 and 5) allow excellent control of the nanotips' size and shape and good control of the spacing, which is on average 10 nm or more in the samples studied. In the films used in this work, each nanotip is about 5–10 nm in diameter at the end, thicker (~60–80 nm in diameter) at the base, and ~0.7 μm long (Figure 1). Both bifunctional acids are about 3 nm long, when considering the chain fully extended, and the length of the FI-dsDNA is about 5 nm. Simple geometrical considerations suggest that the DNA functionalization could occur on most of the upper half of the nanotips surface, but the morphology has clearly an influence on this effect.

We applied the same strategy on two types of sensors: a ZnO nanostructure-based quartz crystal microbalance (nano-QCM)¹⁸ and, more recently, a ZnO-based thin film bulk acoustic resonator.¹⁹ This device allows one to record frequency shifts due to mass loading on its sensing area caused by the piezoelectric effect in the resonator. Details about this device design and function will be published elsewhere.¹⁸ The nanotips ZnO-integrated sensor, because of the dramatic increase of the effective sensing area, exhibited a greatly enhanced performance and sensitivity.¹⁸ This application demonstrated that the selective

immobilization and hybridization of DNA using the strategy described here can be applied to the development of novel nanostructured ZnO sensors.

Experimental Section

Chemicals. 16-(2-Pyridyldithiol)hexadecanoic acid (PDHA) and *N*-(15-carboxypentadecanoyloxy)succinimide (NHS) were synthesized according to previously published procedures.²⁶ Dithiothreitol (DTT) immobilized on polyacrylamide resin (Reductacryl from Calbiochem), DIUF water (Fisher), ethanol, 200 proof (Pharmco), and 1-butanol (Aldrich) were used as received. Freshly prepared 10 mM aqueous PBS buffer (NaCl, KCl, K_2HPO_4 , KH_2PO_4 ; pH 7.4) was used. The choice of the buffer was crucial to avoid etching of the layer.²⁰ The 16 bases 5'-thiol-modified DNA 5'-/5ThioMC6-D/GTGTAGCCTCAAGTG-3' (SH-ssDNA), 16 bases 5'-amino-modified DNA 5'-/5AmMC6/GTGTAGCCTCAAGTG-3' (NH_2 -ssDNA), and complementary 5'-dye(fluorescein)-modified DNA 5'-/56-FAM/CACTTGAGGCTAACAC-3' (ssDNA-FI) were purchased from Integrated DNA Technologies, Inc.

ZnO Nanotip Films. The MOCVD technique was used for the growth of ZnO nanotips with diethylzinc (ZnEt_2) as Zn source, and O_2 as the oxidizer. The substrate temperature was maintained at ~475 $^\circ\text{C}$, and the chamber pressure remained at around 50 Torr during the growth. Such procedures have been described before.²⁷

Spectroscopy. Fluorescence emission spectra were collected on VARIAN Cary-Eclipse. The films were placed diagonally at a 45° angle in a 1 cm cuvette in air while recording the spectra. Attenuated reflectance infrared spectra (FT-IR-ATR) were acquired on a Thermo Electron Corp. Nicolet 6700 FT-IR. Reflection type fluorescence images of the ZnO nanotips grown on c-sapphire substrate were collected with an Axiovert 200 M

(26) (a) Tokutake, N.; Miyake, Y.; Regen, S. L. *Langmuir* **2000**, *16*, 81. (b) Ebashi, I.; Takigawa, T.; Inoue, M. Long chain carboxylic acid imide ester. U.S. Patent 5,414,089, May 9, 1995.

(27) (a) Zhong, J.; Muthukumar, S.; Chen, Y.; Lu, Y.; Ng, H. M.; Jiang, W.; Garfunkel, E. L. *Appl. Phys. Lett.* **2003**, *83*, 16. (b) Zhong, J.; Saraf, G.; Muthukumar, S.; Chen, H.; Chen, Y.; Lu, Y. *TMS IEEE J. Electron. Mater.* **2004**, *33*, 654.

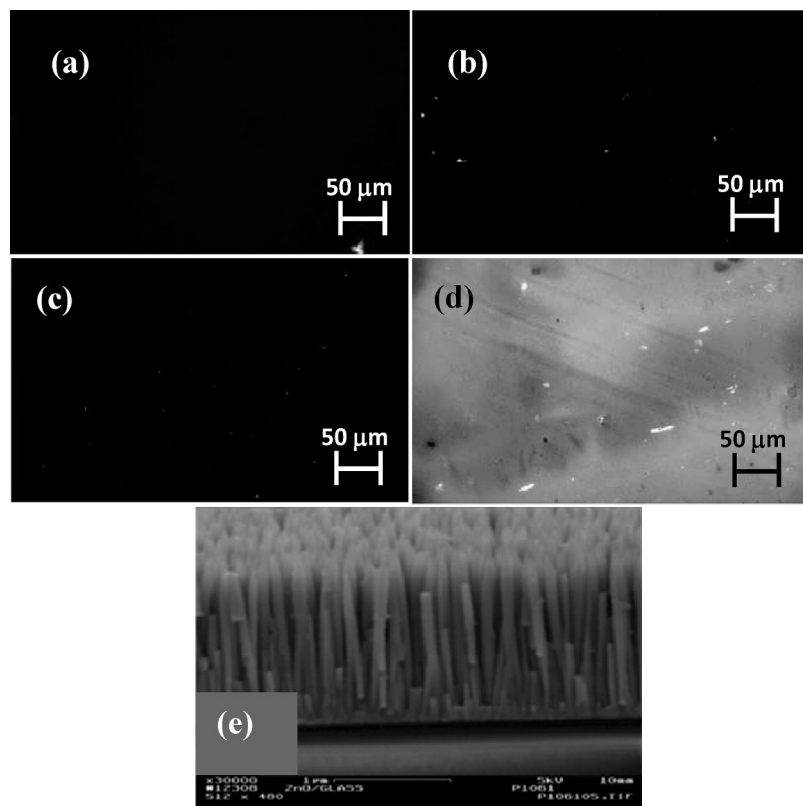


Figure 5. Fluorescence microscopy image of a ZnO nanotips film grown on glass substrate after step 3, sequence A (image d). Only the nanotip films with properly immobilized and hybridized FI-DNA were fluorescing. No fluorescence emission was observed on films after the intermediate steps 1 (image a) and 2 (image b) and in a control experiment where a film after step 1 was treated directly with FI-ssDNA (image c). FESEM image e shows the surface morphology of the ZnO nanotips/glass after the entire functionalization procedure (route A).

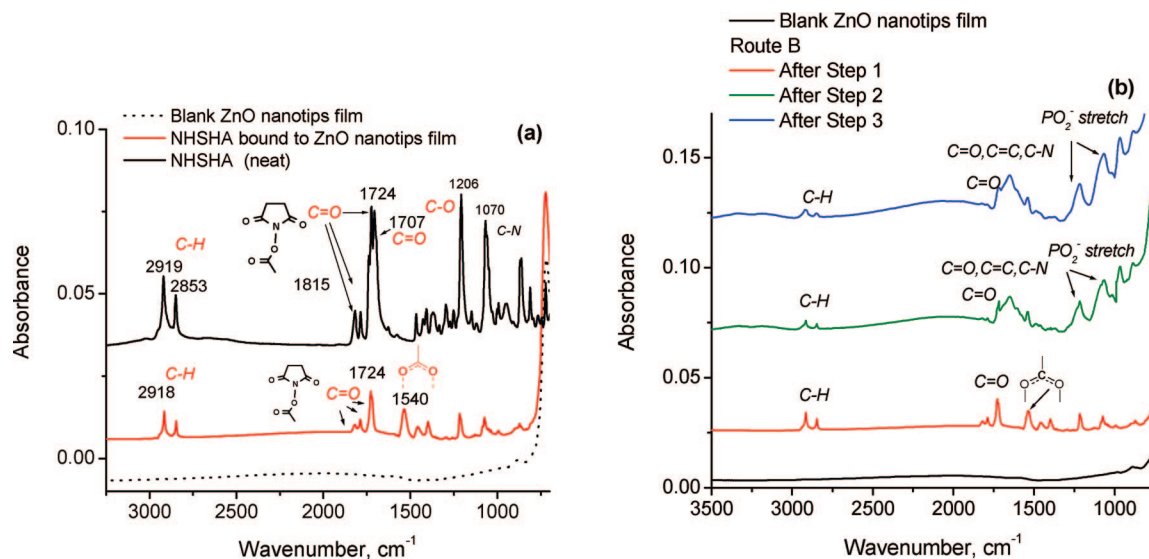


Figure 6. FTIR-ATR spectra of ZnO-N modification process, route B: (a) blank ZnO-N (bottom, dotted line), NHSOA bound to ZnO-N (middle, red solid line), and NHSOA free (top, black solid line), and (b) blank ZnO-N (black line), NHSOA bound to ZnO-N (red line), immobilization of $\text{NH}_2\text{-(CH}_2\text{)}_6\text{-ssDNA}$ (green line), and hybridization with FI-ssDNA (blue line).

confocal fluorescence microscope (Carl Zeiss, Gottingen, Germany) with a 510 nm filter and 480 nm excitation.

Functionalization of ZnO Nanotips Surface. Each step of the ZnO nanotips surface functionalization procedure was performed by immersing the films in a small volume of the indicated solution ($\sim 0.8\text{--}1\text{ mL}$) in a sealed vial to avoid evaporation, at room temperature. After binding for the indicated period of time, the films were thoroughly rinsed with neat solvent and dried under a gentle nitrogen flow. The films were stored for days to weeks in a desiccator and in the dark without apparent change.

Formation of Bifunctional Linker Layer (Route A or B, Step 1). The ZnO nanotip films were immersed in 2 mM PDHA or NHSOA solution in 1-butanol/ethanol 2/1 or neat ethanol, respectively, for 12–15 h. The film was rinsed thoroughly with neat solvent and dried under gentle nitrogen flow.

Immobilization of ssDNA (Route A or B, Step 2). The commercially available thiol-modified ssDNA, which has a thiol in protected form, was reduced with DTT-resin ($\sim 10\text{-fold}$ molar excess) immediately prior to use, to form the free SH groups. The reduction was performed at room temperature for 2 h with periodic shaking

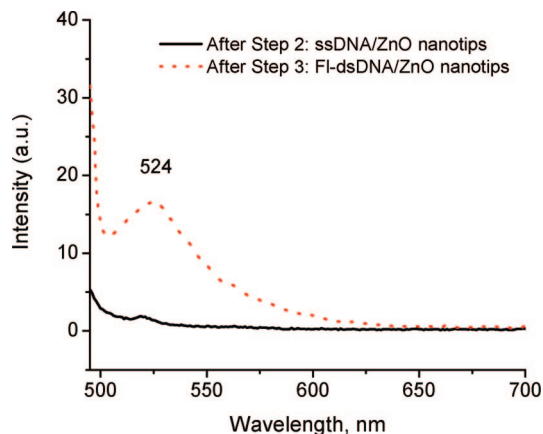


Figure 7. Route B: Fluorescence emission spectra of ZnO-N modified with ssDNA (black line) and ZnO-N with FI-dsDNA (red line). $\lambda_{\text{ex}} = 490$ nm.²⁵

followed by removal of the DTT-resin via filtration through a 0.02 μm membrane syringe filter (Whatman). The films with the reactive layer were immersed in the freshly prepared 25 μM SH-ssDNA (or NH_2 -ssDNA) solution in 10 mM aqueous PBS buffer (pH 7.4) for 4 h in a sealed vial at room temperature. The ZnO film was then rinsed thoroughly with PBS buffer and dried under gentle nitrogen flow.

Hybridization to FI-dsDNA (Route A or B, Step 3). The ssDNA-modified films obtained from step 2 were immersed in 25 μM ssDNA-

FI in 10 mM aqueous PBS buffer for 1.5 h at room temperature. The sample was then rinsed with the buffer solution and dried under gentle nitrogen flow.

Conclusions

A three-step procedure to functionalize ZnO nanotip films with ssDNA, followed by hybridization with complementary and fluorescein-tagged ssDNA, was developed. First, long chain fatty acids capped with two different types of reactive end groups (bifunctional linkers) were bound to the ZnO surface through the COOH group, leaving a second functional group available for further reactions. This allowed one to covalently bind ssDNA to a “reactive layer” on ZnO by two different reactions. A hybridization step was then performed on the DNA-functionalized films. With the three-step procedures for ZnO nanotip functionalization described here, we demonstrated the ability to selectively immobilize DNA molecules, and this method is currently employed to develop ZnO nanotips-integrated biosensors. More importantly, this novel approach allows sequential reactions on the surface of ZnO nanostructures and, in principle, can be extended to numerous other molecules and biomolecules.

Acknowledgment. We are grateful to the Rutgers Research Council for partial support of this work and are indebted to Mr. Oleh Taratula for assistance with DNA hybridization steps.

LA8026946